World Academy of Science, Engineering and Technology
International Journal of Mechanical and Mechatronics Engineering
Vol:9, No:4, 2015

# A TFETI Domain Decompositon Solver for Von Mises Elastoplasticity Model with Combination of Linear Isotropic-Kinematic Hardening

Martin Cermak, Stanislav Sysala



*Abstract*—In this paper we present the efficient parallel implementation of elastoplastic problems based on the TFETI (Total Finite Element Tearing and Interconnecting) domain decomposition method. This approach allow us to use parallel solution and compute this nonlinear problem on the supercomputers and decrease the solution time and compute problems with millions of DOFs. In our approach we consider an associated elastoplastic model with the von Mises plastic criterion and the combination of linear isotropic-kinematic hardening law. This model is discretized by the implicit Euler method in time and by the finite element method in space. We consider the system of nonlinear equations with a strongly semismooth and strongly monotone operator. The semismooth Newton method is applied to solve this nonlinear system. Corresponding linearized problems arising in the Newton iterations are solved in parallel by the above mentioned TFETI. The implementation of this problem is realized in our in-house MatSol packages developed in MatLab.

*Keywords*—Isotropic-kinematic hardening, TFETI, domain decomposition, parallel solution.

## I. Introduction

THE goal of this paper is to present the efficient parallel implementation of elastoplastic problems based on the TFETI (Total Finite Element Tearing and Interconnecting) domain decomposition method [5]. We consider an associated elastoplasticity with the von Mises plastic criterion and the combination of linear isotropic-kinematic hardening law (see e.g. [9], [15], [11]). The corresponding elastoplastic constitutive problem is discretized by the implicit Euler method in time and consequently a nonlinear stress-strain relation is solved by the return mapping concept (see e.g. [15], [1]). This approach leads to solving a nonlinear variational equation with respect to the primal unknown displacement in each time step.

By a finite element space discretization of the one time step problem, we get a system of nonlinear equations. A suitable choice for solution of the nonlinear system is the semismooth Newton method since the strong semismoothness together with other properties ensure local quadratic convergence. Semismooth functions in finite dimensional spaces and the semismooth Newton method were introduced in [16]. Semismoothness in elastoplasticity was investigated for example in [18], [19].

M. Cermak is with the IT4Innovations, VSB - Technical University of Ostrava, 17. listopadu 15/2172, Ostrava, Czech Republic, email: martin.cermak@vsb.cz

S. Sysala is with the Institute of Geonics AS CR, v.v.i., Studentska, Ostrava, Czech Republic, email: stanislav.sysala@ugn.cas.cz

For the linearized system in each Newton iteration, we can use the FETI domain decompositon method, originally introduced by Farhat and Roux [7] and theoretically analyzed by Mandel and Tezaur [13]. In our approach we use modification of FETI method, called TFETI. Hence all subdomain stiffness matrices are singular with a priori known kernels. With known kernel basis we can regularize effectively the stiffness matrix without extra fill in and use any standard sparse Cholesky type decomposition method for nonsingular matrices [2].

In Numerical experiments we will use our in-house software package MatSol [12] developed in Matlab.

## II. Elastoplastic Models

Let us consider a deformable body occupying a domain $\Omega \subset \mathbb{R}^3$ with a Lipschitz continuous boundary $\Gamma = \partial\Omega$. State of the body during the loading process is described by the Cauchy stress tensor $\sigma \in S$, the displacement $u \in \mathbb{R}^3$ and the small strain tensor $\varepsilon \in S$. Here $S = \mathbb{R}^{3\times 3}_{sym}$ is the space of all symmetric second order tensors. More details can be found in [15]. The mentioned variables depend on the spatial variable $x \in \Omega$ and the time variable $t \in [t_0, t^*]$.

Let the boundary $\Gamma$ be fixed on a part $\Gamma_U$ that has a nonzero Lebesgue measure with respect to $\Gamma$, i.e., we prescribe the homogeneous Dirichlet boundary condition on $\Gamma_U$:

$$u(x,t) = 0 \quad \forall (x,t) \in \Gamma_U \times [t_0, t^*]. \tag{1}$$

On the rest of the boundary $\Gamma_N = \Gamma \setminus \Gamma_U$, we prescribe the Neumann boundary conditions

$$\sigma(x,t)n(x) = F(x,t) \quad \forall (x,t) \in \Gamma_N \times [t_0, t^*], \tag{2}$$

where $n(x)$ denotes the exterior unit normal and $F(x,t)$ denotes a prescribed surface forces at the point $x \in \Gamma_N$ and the time $t \in [t_0, t^*]$.

The small strain tensor is related to the displacement by the linear relation

$$\varepsilon(u) = \frac{1}{2}\left(\nabla u + (\nabla u)^T\right). \tag{3}$$

The equilibrium equation has form

$$-\mathrm{div}(\sigma(x,t)) = g(x,t) \quad \forall (x,t) \in \Omega \times [t_0, t^*], \tag{4}$$

where $g(x,t) \in \mathbb{R}^3$ represents the volume force acting at the point $x \in \Omega$ and the time $t \in [t_0, t^*]$.

For a weak formulation of the investigated problem, we introduce the space of kinematically admissible displacements,

$$V = \left\{ v \in [H^1(\Omega)]^3 : \ v = 0 \ \text{ on } \ \Gamma_U \right\}. \tag{5}$$

Then the conditions (4)–(2) can be written in a weak sense by

$$\begin{aligned} &\int_\Omega \langle \sigma, \varepsilon(v) \rangle_F dx = \int_\Omega g^T v dx \\ &\qquad + \int_{\Gamma_N} F^T v ds \quad \forall v \in V, \ \forall t \in [t_0, t^*]. \end{aligned} \tag{6}$$

Here $\varepsilon(v)$ is defined by (3), $\langle ., . \rangle_F$ and $\|.\|_F$ denote the Frobenius scalar product and the corresponding norm on the space $S$, respectively. We assume that the functions $\sigma, F, g$ are sufficiently smooth such that the integrals in (6) are correctly defined in the Lebesgue sense.

The elastoplastic initial-value constitutive model consists of the following components:

1) Additive decomposition of the strain tensor into the elastic and plastic parts:
$$\varepsilon = \varepsilon^e + \varepsilon^p. \tag{7}$$
2) Linear elastic law between the stress and the elastic strain:
$$\sigma = \mathbb{C}\varepsilon^e, \tag{8}$$
where $\mathbb{C}$ is the fourth order tensor.
3) The von Mises yield function coupled with an isotropic hardening variable $\kappa$:
$$\Phi(\sigma, \beta, \kappa) = \sqrt{\frac{3}{2}} \|\text{dev}(\sigma - \beta)\|_F - (\sigma_D + H_m \kappa) \leq 0, \tag{9}$$
where $\sigma_D, H_m > 0$ denote the initial yield stress and the hardening modulus, respectively.
4) The associated plastic flow rule:
$$\dot{\varepsilon}^p = \dot{\gamma} \frac{\partial \Phi}{\partial \sigma} = \dot{\gamma} \sqrt{\frac{3}{2}} \hat{n}(\sigma - \beta), \quad \dot{\gamma} \geq 0, \tag{10}$$
where
$$\hat{n}(\tau - \omega) = \frac{\text{dev}(\tau - \omega)}{\|\text{dev}(\tau - \omega)\|_F}, \quad \tau, \omega \in S, \tag{11}$$
and $\dot{\varepsilon}^p$ and $\dot{\gamma}$ denote the time derivative of the plastic strain and the plastic multiplier, respectively.
5) The kinematic hardening law based on the accumulated plastic strain rate
$$c_0^{-1} \dot{\beta} = -\dot{\gamma} \frac{\partial \Phi}{\partial \beta} = \dot{\gamma} \sqrt{\frac{3}{2}}\, \hat{n}(\sigma - \beta), \tag{12}$$
where $c_0 > 0$ is a linear kinematic hardening modulus.
6) The isotropic hardening law based on the accumulated plastic strain rate:
$$\dot{\kappa} = \sqrt{\frac{2}{3}} \|\dot{\varepsilon}^p\|_F = \dot{\gamma}. \tag{13}$$
Notice that the second equality in (13) follows from (10).
7) The loading/unloading conditions:
$$\dot{\gamma} \geq 0, \ \ \Phi(\sigma, \beta, \kappa) \leq 0, \ \ \dot{\gamma}\Phi(\sigma, \beta, \kappa) = 0. \tag{14}$$
8) The initial conditions:
$$\begin{gathered} \varepsilon(x, t_0) = \varepsilon^e(x, t_0) = \varepsilon^p(x, t_0) = \sigma(x, t_0) = 0 \\ \beta(x, t_0) = 0, \quad \kappa(x, t_0) = 0, \quad x \in \Omega. \end{gathered} \tag{15}$$

## III. Time Discretized Elastoplastic Model

Let us consider the following discretization of the time interval

$$t_0 < t_1 < \ldots < t_k < \ldots < t_N = t^*.$$

Let us denote $\sigma_k = \sigma_k(x) = \sigma(x, t_k)$, $x \in \Omega$ and similarly for other variables. To approximate the time derivatives, we use the implicit Euler method. This method is often used in mathematical and engineering literature, see e.g. [9], [15]. Then by (7) and (8),

$$\begin{aligned} &\dot{\varepsilon}^p(t_{k+1}) \approx \tfrac{\varepsilon^p_{k+1} - \varepsilon^p_k}{\triangle t_{k+1}} = \tfrac{\mathbb{C}^{-1}(\sigma^t_{k+1} - \sigma_{k+1})}{\triangle t_{k+1}}, \\ &\triangle t_{k+1} = t_{k+1} - t_k, \end{aligned} \tag{16}$$

where

$$\sigma^t_{k+1} := \sigma_k + \mathbb{C} \triangle \varepsilon_{k+1}, \quad \triangle \varepsilon_{k+1} = \varepsilon_{k+1} - \varepsilon_k. \tag{17}$$

Here $\sigma^t_{k+1}$ is the trial stress tensor. By (7)–(17), we can formulate the time discretized elastoplastic *constitutive* problem as follows. Given the values $\sigma_k$, $\beta_k$, $\kappa_k$, $\varepsilon_k$ of the stress, the kinematic hardening, the isotropic hardening, and the strain, respectively, at the time $t_k$ and given the incremental strain $\triangle \varepsilon_{k+1}$ for the interval $[t_k, t_{k+1}]$, solve the following system of algebraic equations

$$\mathbb{C}^{-1}(\sigma^t_{k+1} - \sigma_{k+1}) = \triangle \gamma_{k+1} \sqrt{\frac{3}{2}}\, \hat{n}(\sigma_{k+1} - \beta_{k+1}) \tag{18}$$

$$c_0^{-1}(\beta_{k+1} - \beta_k) = \triangle \gamma_{k+1} \sqrt{\frac{3}{2}}\, \hat{n}(\sigma_{k+1} - \beta_{k+1}) \tag{19}$$

$$\kappa_{k+1} - \kappa_k = \triangle \gamma_{k+1} \tag{20}$$

for the unknowns $\sigma_{k+1}$, $\beta_{k+1}$, $\kappa_{k+1}$, and $\triangle \gamma_{k+1}$, subject to the constraints

$$\begin{gathered} \triangle \gamma_{k+1} \geq 0, \ \ \Phi(\sigma_{k+1}, \beta_{k+1}, \kappa_{k+1}) \leq 0, \\ \triangle \gamma_{k+1} \Phi(\sigma_{k+1}, \beta_{k+1}, \kappa_{k+1}) = 0. \end{gathered} \tag{21}$$

This constitutive problem can be solved explicitly by the return mapping concept (see e.g. [1], [15]). It means that we firstly verify whether $\Phi(\sigma^t_{k+1}, \beta_k, \kappa_k) \leq 0$ (elastic predictor). If this inequality holds then

$$\begin{gathered} \triangle \gamma_{k+1} = 0, \quad \sigma_{k+1} = \sigma^t_{k+1}, \quad \triangle \sigma_{k+1} = \mathbb{C} \triangle \varepsilon_{k+1}, \\ \beta_{k+1} = \beta_k, \quad \kappa_{k+1} = \kappa_k, \end{gathered} \tag{22}$$

is the solution of the discretized constitutive problem. Conversely, $\Phi(\sigma^t_{k+1}, \beta_k, \kappa_k) > 0$, then by the plastic corrector we obtain

$$\begin{aligned} &\triangle \gamma_{k+1} = \tfrac{2}{3} \tfrac{1}{\alpha} \Phi_k, \\ &\sigma_{k+1} = \sigma^t_{k+1} - \tfrac{2\mu}{\alpha} \sqrt{\tfrac{2}{3}} \Phi_k \hat{n}_k, \\ &\beta_{k+1} = \beta_k + \tfrac{c_0}{\alpha} \sqrt{\tfrac{2}{3}} \Phi_k \hat{n}_k, \\ &\kappa_{k+1} = \kappa_k + \tfrac{2}{3\alpha} \Phi_k, \end{aligned} \tag{23}$$

where

$$\Phi_k = \Phi(\sigma^t_{k+1}, \beta_k, \kappa_k),$$

$$\hat{n}_k = \hat{n}(\sigma^t_{k+1} - \beta_k),$$

$$\alpha = 2\mu + c_0 + \tfrac{2}{3}H_m.$$

Notice that the second and third formulas in (23) are correctly defined since the denominator $\|\mathrm{dev}(\sigma^t_{k+1} - \beta_k)\|_F > 0$ for $\Phi(\sigma^t_{k+1}, \beta_k, \kappa_k) > 0$. Let us define the stress and hardening operators $T_{\sigma,k} : S \to S$, $T_{\beta,k} : S \to S$, $T_{\kappa,k} : S \to \mathbb{R}$ such that for $\eta \in S$

$$T_{\sigma,k}(\eta) := \mathbb{C}\eta - \frac{2\mu}{\alpha}\sqrt{\frac{2}{3}}\Phi^+_k\hat{n}_k, \quad (24)$$

$$T_{\beta,k}(\eta) := \frac{c_0}{\alpha}\sqrt{\frac{2}{3}}\Phi^+_k\hat{n}_k, \quad (25)$$

$$T_{\kappa,k}(\eta) := \frac{2}{3\alpha}\Phi^+_k, \quad (26)$$

respectively, where $\Phi^+$ denotes the positive part of the function $\Phi$. Then by (17), (20), (22), (23), (24), (25), and (26),

$$\begin{aligned} \triangle\beta_{k+1} &= T_{\beta,k}(\triangle\varepsilon_{k+1}), \\ \triangle\kappa_{k+1} &= T_{\kappa,k}(\triangle\varepsilon_{k+1}), \\ \triangle\sigma_{k+1} &= T_{\sigma,k}(\triangle\varepsilon_{k+1}). \end{aligned} \quad (27)$$

By [1], [19], the operator $T_{\sigma,k} : S \to S$ is potential, Lipschitz continuous, strongly monotone, and strongly semismooth on $S$.

Let us note that semismoothness was originally introduced by Mifflin [14] for functionals. Qi and J. Sun [16] extended the definition of semismoothness to vector-valued function to investigate the superlinear convergence of the Newton method. The strong semismoothness of the Lipschitz continuous function $T_{\sigma,k}(.)$ means that $T_{\sigma,k}(.)$ is directionally differentiable on $S$ and has a quadratic approximate property at any $\eta \in S$, i.e., for any $\xi \in S$, $\xi \to 0$, and any $T^o_{\sigma,k}(\eta+\xi) \in \partial T_{\sigma,k}(\eta+\xi)$,

$$T_{\sigma,k}(\eta+\xi) - T_{\sigma,k}(\eta) - T^o_{\sigma,k}(\eta+\xi)\xi = O(\|\xi\|^2_F). \quad (28)$$

Here $\partial T_{\sigma,k}(\eta+\xi)$ denotes the set of the Clark generalized derivatives of $T_{\sigma,k}$ at $\eta+\xi$. Then we can choose the Clark generalized derivative $T^o_{\sigma,k}$ of $T_{\sigma,k}$ in the following way:

1. If $\Phi_k \le 0$, then

$$T^o_{\sigma,k}(\eta) = \mathbb{C}. \quad (29)$$

2. If $\Phi_k > 0$, then

$$T^o_{\sigma,k}(\eta) = \mathbb{C} - \frac{2\mu}{\alpha}\sqrt{\frac{2}{3}}\left(\hat{n}_k \otimes \frac{\partial\Phi_k}{\partial\eta} + \Phi_k\frac{\partial\hat{n}_k}{\partial\eta}\right), \quad (30)$$

where

$$\begin{aligned} \frac{\partial\Phi_k}{\partial\eta} &= 2\mu\sqrt{\frac{3}{2}}\,\hat{n}_k, \\ \frac{\partial\hat{n}_k}{\partial\eta} &= 2\mu\frac{\mathbb{I}_d - \hat{n}_k\otimes\hat{n}_k}{\|\mathrm{dev}(\sigma_k + \mathbb{C}\eta - \beta_k)\|_F}, \\ \mathbb{I}_d\xi &:= \mathrm{dev}(\xi), \quad \forall\xi \in S. \end{aligned}$$

Notice that $T_{\sigma,k}$ is not differentiable at $\eta \in S$, $\Phi_k = 0$. Otherwise $T^o_{\sigma,k}(\eta) = \partial T_{\sigma,k}(\eta)/\partial\eta$.

Let us recall that the stress, strain, kinematic hardening, isotropic hardening, and displacement variables also depend on a spatial variable $x \in \Omega$. We consider the dependence of $T_{\sigma,k}(\triangle\varepsilon_k)$ on $x$ in the following sense:

$$T_{\sigma,k}(\triangle\varepsilon_k) = T_{\sigma,k}(\triangle\varepsilon_k)(x). \quad (31)$$

Then we can substitute the stress operator $T_{\sigma,k}$, defined by (24), into the balance equation (6) to obtain the time discretized elastoplastic problem in the incremental form.

*Problem 1: Given the stress field $\sigma_k \in [L^2(\Omega)]^{3\times3}_{sym}$, the kinematic hardening field $\beta_k \in [L^2(\Omega)]^{3\times3}_{sym}$, and the isotropic hardening field $\kappa_k \in L^2(\Omega)$ at the time $t_k$, find the displacement $u_{k+1} = u_k + \triangle u_{k+1} \in V$, where the increment $\triangle u_{k+1} \in V$ solves the variational equation*

$$\begin{aligned} &\int_\Omega \langle T_{\sigma,k}(\varepsilon(\triangle u_{k+1})), \varepsilon(v)\rangle_F dx = \int_\Omega \triangle g^T_{k+1} v dx \\ &\quad + \int_{\Gamma_N} \triangle F^T_{k+1} v ds \quad \forall v \in V, \end{aligned} \quad (32)$$

*with loading increments $\triangle F_{k+1} = F_{k+1} - F_k$, $\triangle g_{k+1} = g_{k+1} - g_k$. Set the stress, kinematic hardening, and isotropic hardening fields $\sigma_{k+1} = \sigma_k + \triangle\sigma_{k+1}$, $\beta_{k+1} = \beta_k + \triangle\beta_{k+1}$, $\kappa_{k+1} = \kappa_k + \triangle\kappa_{k+1}$ in the next time step $t_{k+1}$ from the relations*

$$\begin{aligned} \triangle\sigma_{k+1} &= T_{\sigma,k}(\varepsilon(\triangle u_{k+1})), \\ \triangle\beta_{k+1} &= T_{\beta,k}(\varepsilon(\triangle u_{k+1})), \\ \triangle\kappa_{k+1} &= T_{\kappa,k}(\varepsilon(\triangle u_{k+1})), \end{aligned} \quad (33)$$

*almost everywhere in $\Omega$.*

Problem 1 can be equivalently formulated as a minimization problem [18]. Since the operator $T_{\sigma,k}$ is strongly monotone and Lipschitz continuous on $S$, the non-linear equation (32) has a unique solution $\triangle u_{k+1} \in V$ (see e.g. [8]).

We assume a polyhedral 3D domain $\Omega$ and use the linear simplex elements. We get this nonlinear equation

$$\begin{aligned} &\text{find } \triangle\boldsymbol{u}_{k+1} \in \boldsymbol{V}: \\ &\boldsymbol{v}^T\left(\boldsymbol{F}_k(\triangle\boldsymbol{u}_{k+1}) - \triangle\boldsymbol{f}_{k+1}\right) = 0 \quad \forall\boldsymbol{v} \in \boldsymbol{V}, \end{aligned} \quad (34)$$

where $\triangle\boldsymbol{f}_{k+1}$ is the increment of the load vector, $\boldsymbol{F}_k$ is a nonlinear operator, and space $\boldsymbol{V}$ is the set of admissible displacements

$$\boldsymbol{V} := \{\boldsymbol{v} \in \mathbb{R}^n | \boldsymbol{B}_U\boldsymbol{v} = \boldsymbol{o}\}.$$

The relation $\boldsymbol{B}_U\boldsymbol{v} = \boldsymbol{o}$ represents Dirichlet boundary conditions.

The non-linear system of Equation (34) is solved by the semismooth Newton method and in the each Newton iteration we solved this problem

$$\begin{aligned} &\text{find } \boldsymbol{\delta u}_i \in \boldsymbol{V}: \\ &\boldsymbol{v}^T\left(\boldsymbol{K}_{k,i}\boldsymbol{\delta u}_i - \triangle\boldsymbol{f}_{k+1} + \boldsymbol{F}_k(\triangle\boldsymbol{u}_{k,i})\right) = 0 \quad \forall\boldsymbol{v} \in \boldsymbol{V}, \end{aligned} \quad (35)$$

and compute new approximation of displacement

$$\triangle\boldsymbol{u}_{k,i+1} = \triangle\boldsymbol{u}_{k,i} + \boldsymbol{\delta u}_i.$$

The problem (35) can be also equivalently rewritten as a minimization problem:

$$\text{find } \boldsymbol{\delta u}_i \in \boldsymbol{V}: \quad \boldsymbol{J}(\boldsymbol{\delta u}_i) \le \boldsymbol{J}(\boldsymbol{v}),\ \forall\boldsymbol{v} \in \boldsymbol{V}, \quad (36)$$

where

$$\boldsymbol{J}(\boldsymbol{v}) = \frac{1}{2}\boldsymbol{v}^T\boldsymbol{K}_{k,i}\boldsymbol{v} - \left(\triangle \boldsymbol{f}_{k+1} - \boldsymbol{F}_k(\boldsymbol{v})\right)^T \boldsymbol{v}, \quad \boldsymbol{v} \in \boldsymbol{V}. \tag{37}$$

## IV. TFETI Domain Decompositon Method

The system (36) of linear equations can be solved by the TFETI domain decompositon method.

The basic difference between the original FETI method [7], [6] and TFETI [5] is that all subdomains are kept floating and Dirichlet boundary conditions are enforced by means of a constraint matrix and Lagrange multipliers, similarly to the gluing conditions along subdomain interfaces. This simplifies implementation of the stiffness matrix pseudoinverse. The main advantages is that the local stiffness matrices can by effectively regularized and their kernels are known a priori [2], have the same dimension and can be formed directly from mesh data.

Let us consider a partition of the global domain $\Omega$ into $N_S$ subdomains $\Omega^s, s = 1, \ldots, N_S$. We assign to each subdomain $\Omega^s$ the stiffness matrix $\mathbf{K}^s$ and the nodal load vector $\mathbf{f}^s$. Objects $\mathbf{K}^s$ and $\mathbf{f}^s$ are altered in each Newton iteration. The matrix $\mathbf{K}^s$ represents the tangential symmetric and positive semidefinite stiffness matrix of the subdomain $\Omega^s$. The vector $\mathbf{f}^s$ represents the increment of right hand side minus nonlinear operator $\boldsymbol{F}_k$ from equation (37) for the given subdomain $s$. $\mathbf{R}^s$ shall be a matrix whose columns span the nullspace (kernel) of $\mathbf{K}^s$. Let $\mathbf{B}^s$ be a signed boolean matrix defining connectivity of the subdomain $s$ with neighbour subdomains, it also enforces Dirichlet boundary conditions when TFETI is used. They constitute global objects

$$\begin{aligned}
\mathbf{K} &= \mathrm{diag}(\mathbf{K}^1, \ldots, \mathbf{K}^{N_S}) \in \mathbb{R}^{N_p \times N_p},\\
\mathbf{R} &= \mathrm{diag}(\mathbf{R}^1, \ldots, \mathbf{R}^{N_S}) \in \mathbb{R}^{N_p \times N_n},\\
\mathbf{B} &= [\mathbf{B}^1, \ldots, \mathbf{B}^{N_S}] \in \mathbb{R}^{N_d \times N_p},\\
\mathbf{f} &= [(\mathbf{f}^1)^T, \ldots, (\mathbf{f}^{N_S})^T]^T \in \mathbb{R}^{N_p \times 1},
\end{aligned}$$

where $N_p, N_d, N_n$ denote the primal dimension, the dual dimension, and the null space dimension, respectively. Primal dimension means the number of all DOFs including those arising from duplication on the interfaces. Dual dimension is the total number of equality constraints. Note that columns of $\mathbf{R}$ also span the kernel of $\mathbf{K}$, and $\mathbf{K}$ is a symmetric and positive semidefinite matrix.

Let us apply the duality theory to the primal problem (36)

$$\min \frac{1}{2}\mathbf{u}^T\mathbf{K}\mathbf{u} - \mathbf{u}^T\mathbf{f} \quad \text{s.t.} \quad \mathbf{B}\mathbf{u} = \mathbf{o} \tag{38}$$

and establish the notation

$$\mathbf{F} = \mathbf{B}\mathbf{K}^\dagger\mathbf{B}^T, \quad \mathbf{G} = \mathbf{R}^T\mathbf{B}^T, \quad \mathbf{d} = \mathbf{B}\mathbf{K}^\dagger\mathbf{f}, \quad \mathbf{e} = \mathbf{R}^T\mathbf{f}.$$

$\mathbf{K}^\dagger$ denotes a pseudoinverse (generalized inverse) of $\mathbf{K}$, satisfying $\mathbf{K}\mathbf{K}^\dagger\mathbf{K} = \mathbf{K}$, and $\mathbf{G}$ is a so-called *natural coarse space matrix*. We obtain a new minimization problem

$$\min \frac{1}{2}\boldsymbol{\lambda}^T\mathbf{F}\boldsymbol{\lambda} - \boldsymbol{\lambda}^T\mathbf{d} \quad \text{s.t.} \quad \mathbf{G}\boldsymbol{\lambda} = \mathbf{e}. \tag{39}$$

Equality constraints $\mathbf{G}\boldsymbol{\lambda} = \mathbf{e}$ can be homogenized by splitting $\boldsymbol{\lambda}$ into $\boldsymbol{\mu} + \widetilde{\boldsymbol{\lambda}}$ where $\widetilde{\boldsymbol{\lambda}}$ satisfies $\mathbf{G}\widetilde{\boldsymbol{\lambda}} = \mathbf{e}$ (e.g. $\widetilde{\boldsymbol{\lambda}} = \mathbf{G}^T(\mathbf{G}\mathbf{G}^T)^{-1}\mathbf{e}$) and $\boldsymbol{\mu} \in \mathrm{Ker}\,\mathbf{G}$. The homogenized problem reads as follows:

$$\min \frac{1}{2}\boldsymbol{\mu}^T\mathbf{F}\boldsymbol{\mu} - \boldsymbol{\mu}^T\widetilde{\mathbf{d}} \quad \text{s.t.} \quad \mathbf{G}\boldsymbol{\mu} = \mathbf{o}, \tag{40}$$

where $\widetilde{\mathbf{d}} = \mathbf{d} - \mathbf{F}\widetilde{\boldsymbol{\lambda}}$. Furthermore, the constraints $\mathbf{G}\boldsymbol{\mu} = \mathbf{o}$ can be enforced by the projector $\mathbf{P}_\mathbf{G}$ onto the null space of $\mathbf{G}$:

$$\mathbf{P}_\mathbf{G} = \mathbf{I} - \mathbf{Q}, \quad \mathbf{Q} = \mathbf{G}^T\mathbf{H}\mathbf{G}, \quad \mathbf{H} = (\mathbf{G}\mathbf{G}^T)^{-1}.$$

It holds $\mathrm{Im}\,\mathbf{P}_\mathbf{G} = \mathrm{Ker}\,\mathbf{G}$, $\mathrm{Im}\mathbf{G} = \mathrm{Im}\mathbf{G}^T$. We call the action of $\mathbf{H}$ the *coarse problem* of FETI. By these means, the equality constraints are incorporated into the objective function, and we get an unconstrained minimation problem

$$\min \frac{1}{2}\boldsymbol{\mu}^T\mathbf{P}_\mathbf{G}\mathbf{F}\mathbf{P}_\mathbf{G}\boldsymbol{\mu} - \boldsymbol{\mu}^T\mathbf{P}_\mathbf{G}\widetilde{\mathbf{d}}. \tag{41}$$

Finally, the unconstrained minimization problem can be written as a linear system. It holds that $\mathbf{P}_\mathbf{G}\boldsymbol{\mu} = \boldsymbol{\mu}$ for any $\boldsymbol{\mu} \in \mathrm{Ker}\,\mathbf{G}$. We can therefore omit one action of $\mathbf{P}_\mathbf{G}$. The final problem reads

$$\mathbf{P}_\mathbf{G}\mathbf{F}\boldsymbol{\mu} = \mathbf{P}_\mathbf{G}\widetilde{\mathbf{d}}. \tag{42}$$

Problem (42) can be solved with an arbitrary iterative linear system solver. The conjugate gradient (CG) method is a good choice thanks to the classical estimate of the spectral condition number by Farhat, Mandel and Roux [6]:

$$\kappa(\mathbf{P}_\mathbf{G}\mathbf{F}\mathbf{P}_\mathbf{G}|\mathrm{Im}\mathbf{P}_\mathbf{G}) \leq C\frac{H}{h}. \tag{43}$$

More details about TFETI and elastoplasticity can be found in [4], [3].

## V. Numerical Experiments

All numerical experiments were performed using Anselm supercomputer located at IT4Innovations, Ostrava, Czech Republic. The Anselm cluster consists of 209 compute nodes, totaling 3344 compute cores with 15 TB of RAM and giving a theoretical peak performance of over 94 Tflop/s. Each node is a powerful x86-64 computer, equipped with 16 cores, at least 64GB RAM, and 500GB harddrive. Nodes are interconnected by fully non-blocking fat-tree Infiniband network and equipped with Intel Sandy Bridge processors.

The proposed algorithms were implemented in `MatSol` library [12] developed in Matlab and parallelized using Matlab Distributed Computing Server and Matlab Parallel Toolbox. The MatSol library allow us to use parallel algorithm for solving linearized problem by TFETI. The alternative software package is PERMON [10], which is implemented in PETSc [17]. PERMON is in progress nowadays.

The performance of our approach is demonstrated on an elastoplastic homogeneous cube of sizes $1 \times 1 \times 1$ dm (see Fig. 1). The cube is fixed on the lower face ($z = 0$) and Neuman boundary condition in the form $g(t) = p_z = \sin(500t)$ MPa are prescribed on the upper face ($z = 1$). We consider the time interval $[0, 1]$ and divide it into $40$ time steps. Fig. 1 also depicts one of the considered decomposition and the meaning of the discretization parameter $h$ and the decomposition parameter $H$. The elastoplastic body $\Omega$ is made from the

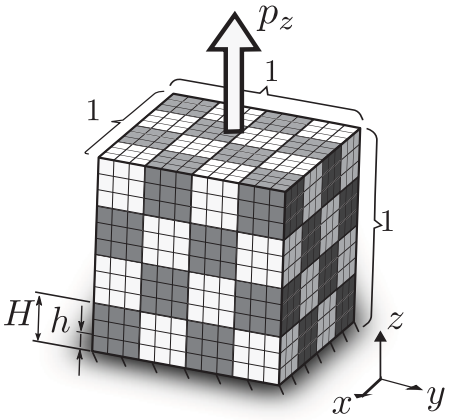


Fig. 1. Geometry.

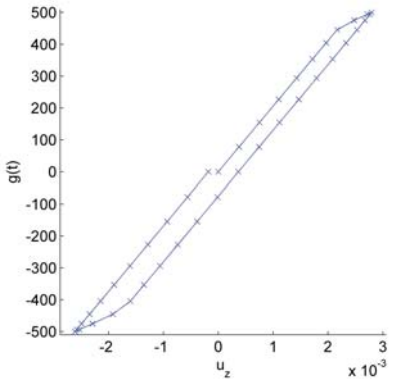


Fig. 2. Hysteresis curve for $M = 0.25$.

homogeneous isotropic material with parameters $E = 200$ GPa, $\nu = 0.33$, $\sigma_y = 450$ MPa, $H_m = M \cdot 100$ GPa, and $c_0 = (1 - M) \cdot 2/3 H_m$ where $E$ and $\nu$ are the Young modulus and the Poisson ratio, respectively. Here $M \in [0, 1]$ is a weight variable which allow us change behaviour of our model. It means that, in the case $M = 0$ we have only kinematic hardening and for case $M = 1$ we get only isotropic hardening.

To test numerical scalability, the domain $\Omega$ was partitioned regularly from $2^3 = 8$ to $8^3 = 512$ subdomains. The parameter $N = N_x = N_y = N_z$ described the number of subdomains in $x$ direction, in $y$ and $z$ directions as well. We kept the constant number $N_p^s = 3,993$ of primal variables per subdomain and the number of subdomains per core is also constant and set to 4. Therefore the total number of primal variables ranges from $27,783$ to $1,594,323$. The stopping tolerances of the Newton and the CG algorithms are $\epsilon_{Newton} = 10^{-4}$ and $\epsilon_{CG} = 10^{-8}$. The other detail about problem setting can be found in the Table I.

The examples of hysteresis curves are in Fig. 2 and Fig. 3. These hysteresis curves represent dependence of displacement in $z$ - th direction on the surface forces. It was chosen the node with $[0.0; 0.0; 1.0]$ coordinates and was drawn for the problem with the finest meshes.

In Tables II - V can be found the main results for

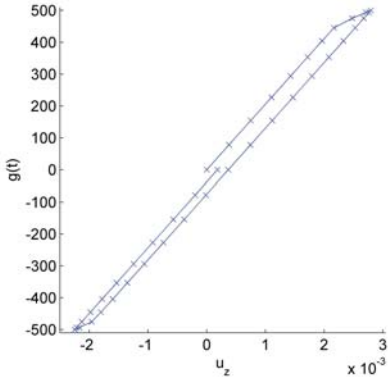


Fig. 3. Hysteresis curve for $M = 0.75$.

TABLE I
PROBLEM SETTING

| N | 2 | 4 | 6 | 8 |
|---|---|---|---|---|
| No. of subdomains | 8 | 64 | 216 | 512 |
| No. of cores | 3 | 17 | 55 | 129 |
| No. of elements | 48,000 | 384,000 | 1,296,000 | 3,072,000 |
| Primal variables | 27,783 | 206,763 | 680,943 | 1,594,323 |

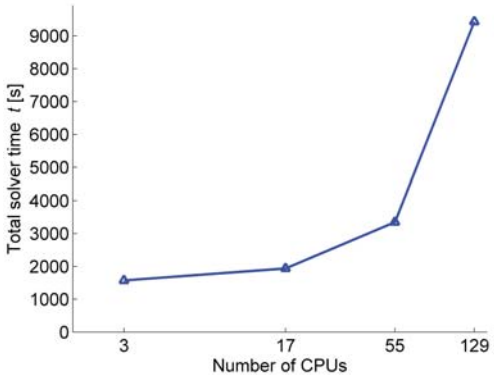


Fig. 4. Weak parallel scalability.

chosen decomposition of our benchmark and different values of variable $M$. We observe the numbers of the Newton and CG iterations are highest for $M = 0$ (only kinematic hardening) and gradually decreases with increasing $M$. This also corresponds with decreasing time of solution. We can also see that the total time is only five times greater for $N = 8$ that for $N = 2$.

Fig. 4 and Fig. 5 depicts weak parallel scalability and numerical scalability, respectively. In Fig. 4 we see that the solution time grows up. On the other hand, from Fig. 5 we observe that the total number of CG iterations grows up only moderately.

## VI. CONCLUSION

We proposed the algorithm which is efficient for parallel implementation of elastoplastic problems. The performance of our algorithm was demonstrated on the 3D elastoplastic unit cube with prescribed loading history. Numerical results for different mesh levels were presented and discussed. The graph

TABLE II
RESULT FOR THE DECOMPOSITION GIVEN BY $N = 8$ AND DIFFERENT VALUES OF $M$.

| M | 0.00 | 0.25 | 0.50 | 0.75 | 1.00 |
|---|---|---|---|---|---|
| Tot. No. of New. iter. | 111 | 106 | 105 | 104 | 102 |
| Tot. No. of CG iters. | 5,016 | 4,781 | 4,728 | 4,661 | 4,537 |
| Tot. solver time [s] | 10,047 | 9,455 | 9,431 | 9,380 | 9,191 |
| Tot. time [s] | 13,02 | 12,42 | 12,33 | 12,28 | 11,95 |

TABLE III
RESULT FOR THE DECOMPOSITION GIVEN BY $N = 6$ AND DIFFERENT VALUES OF $M$.

| M | 0.00 | 0.25 | 0.50 | 0.75 | 1.00 |
|---|---|---|---|---|---|
| Tot. No. of New. iter. | 111 | 108 | 107 | 106 | 104 |
| Tot. No. of CG iters. | 4,988 | 4,841 | 4,792 | 4,729 | 4,596 |
| Tot. solver time [s] | 3,442 | 3,397 | 3,347 | 3,303 | 3,230 |
| Tot. time [s] | 5,073 | 5,008 | 4,939 | 4,879 | 4,722 |

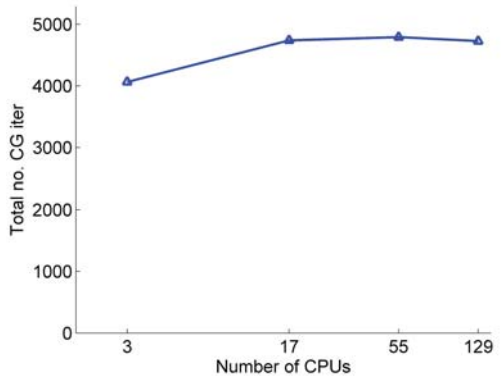


Fig. 5. Numerical scalability.

of weak parallel scalability shows the solution time would be better. On the other hand the graph of numerical scalability is very promising.

## ACKNOWLEDGMENT

The authors acknowledge the support of the project POSTDOCI II reg. no. CZ.1.07/2.3.00/30.0055 within Operational Programme Education for Competitiveness, the Grant Agency of the Czech Republic (GACR) 13-18652S. The work was also supported the European Regional Development Fund in the IT4Innovations Centre of Excellence project (CZ.1.05/1.1.00/02.0070) and the Project of major infrastructures for research, development and innovation of Ministry of Education, Youth and Sports with reg. num. LM2011033.

TABLE IV
RESULT FOR THE DECOMPOSITION GIVEN BY $N = 4$ AND DIFFERENT VALUES OF $M$.

| M | 0.00 | 0.25 | 0.50 | 0.75 | 1.00 |
|---|---|---|---|---|---|
| Tot. No. of New. iter. | 112 | 110 | 108 | 107 | 104 |
| Tot. No. of CG iters. | 4,941 | 4,839 | 4,739 | 4,711 | 4,515 |
| Tot. solver time [s] | 2,007 | 1,972 | 1,936 | 1,929 | 1,869 |
| Tot. time [s] | 3,227 | 3,178 | 3,123 | 3,115 | 2,998 |

TABLE V
RESULT FOR THE DECOMPOSITION GIVEN BY $N = 2$ AND DIFFERENT VALUES OF $M$.

| M | 0.00 | 0.25 | 0.50 | 0.75 | 1.00 |
|---|---|---|---|---|---|
| Tot. No. of New. iter. | 108 | 107 | 105 | 105 | 102 |
| Tot. No. of CG iters. | 4,207 | 4,155 | 4,064 | 4,054 | 3,896 |
| Tot. solver time [s] | 1,593 | 1,556 | 1,572 | 1,538 | 1,442 |
| Tot. time [s] | 2,643 | 2,588 | 2,600 | 2,561 | 2,394 |

## REFERENCES

[1] R. Blaheta, *Numerical methods in elasto-plasticity*, Documenta Geonica 1998, PERES Publishers, Prague, 1999.
[2] T. Brzobohaty, Z. Dostal, P. Kovar, T. Kozubek, A. Markopoulos, *Cholesky decomposition with fxing nodes to stable evaluation of a generalized inverse of the stiffness matrix of a floating structure*, Int. J. Numer. Methods Eng. 88 (5), 493–509, 2011.
[3] M. Cermak, T. Kozubek, *An efficient TFETI based solver for elasto-plastic problems of mechanics*, Advances in Electrical and Electronic Engineering 10 (1), 57–62, 2012.
[4] M. Cermak, T. Kozubek, S. Sysala, J. Valdman, *A TFETI domain decomposition solver for elastoplastic problems*, Appl. Math. and Comput. 231, 634–653, 2014.
[5] Z. Dostál, D. Horák, R. Kučera, *Total FETI - an easier implementable variant of the FETI method for numerical solution of elliptic PDE*, Commun. Numer. Methods Eng. 22 (12), 1155–1162, 2006.
[6] C. Farhat, J. Mandel, F-X. Roux, *Optimal convergence properties of the FETI domain decomposition method*, Comput. Meth. Appl. Mech. Eng. 115, 365–385, 1994.
[7] C. Farhat, F-X. Roux, *A method of finite element tearing and interconnecting and its parallel solution algorithm*, Int. J. Numer. Methods Eng. 32, 1205–1227, 1991.
[8] S. Fučík, A. Kufner, *Nonlinear Differential Equation*, Elsevier, 1980.
[9] W. Han, B. D. Reddy, *Plasticity: mathematical theory and numerical analysis*, Springer, 1999.
[10] V. Hapla et al: FLLOP Web Page. [Online]. Available: http://industry.it4i.cz/en/products/permon/
[11] A. Kossa, L. Szabó, *Exact integration of the von Mises elastoplasticity model with combined linear isotropic-kinematic hardening*, International Journal of Plasticity 25, 1083–1106, 2009.
[12] T. Kozubek, A. Markopoulos, T. Brzobohatý, R. Kučera, V. Vondrák, Z. Dostál, *MatSol - MATLAB efficient solvers for problems in engineering*, http://matsol.vsb.cz/
[13] J. Mandel, R. Tezaur, *Convergence of a substructuring method with Lagrange multipliers*, Numer. Math. 73, 473–487, 1996.
[14] R. Mifflin, *Semismoothness and semiconvex function in constraint optimization*, SIAM J. Cont. Optim. 15, 957–972, 1977.
[15] E. A. de Souza Neto, D. Perić, D. R. J. Owen, *Computational methods for plasticity: theory and application.* Wiley, 2008.
[16] L. Qi, J. Sun, *A nonsmooth version of Newton' s method*, Math. Progr., 58, 353–367, 1993.
[17] B.F. Smith et al: PETSc Web page. [Online]. Available: `http://www.mcs.anl.gov/petsc/`
[18] S. Sysala, *Application of a modified semismooth Newton method to some elasto-plastic problems.* Math. Comput. Simul. 82, 2004–2021, 2012.
[19] S. Sysala, *Properties and simplifications of constitutive time-discretized elastoplastic operators*. Z. Angew. Math. Mech., 1–23, 2013.

**Martin Cermak** Martin Cermak was born in 1983 in Hranice, graduated from the Faculty of Electrical Engineering and Computer Science of the VSB-Technical University of Ostrava in 2008 in the field of Interface between COMSOL and OOSol for Solving Contact Problems. He completed his PhD studies in the field of Scalable algorithms for solving elasto-plastic problems in 2012. Currently he is a junior researcher at the IT4Innovations National Supercomputing Center. His current research interests concern mainly the TFETI domain decomposition, parallel implementation, and elastoplastic problems for equality and inequality.